AD NUMBER

AD904302

NEW LIMITATION CHANGE

TO

Approved for public release, distribution unlimited

FROM

Distribution authorized to U.S. Gov't. agencies only; Test and Evaluation; SEP 1972. Other requests shall be referred to Air Force Weapons Laboratory, ATTN: DEV, Kirtland AFB, NM 87117.

AUTHORITY

AFWL ltr dtd 6 Feb 1974

AFWL-TR-72-118

# PRELIMINARY TESTS ON CELLULAR CONCRETE FOR SMALL-SCALE CRATERING STUDIES.

Hans Engle

Dale E. Stephenson

University of New Mexico, CERF



TECHNICAL REPORT, NO. AFWL-TR-72-118

Jun 71 - Mar 72.

Sep 72

AIR FORCE WEAPONS LABORATORY
Air Force Systems Command
Kirtland Air Force Base
New Mexico



Distribution limited to US Government agencies only because test and evaluation information is discussed in the report (Sep 72). Other requests for this document must be referred to AFWL (DEV), Kirtland AFB, NM, 87117.

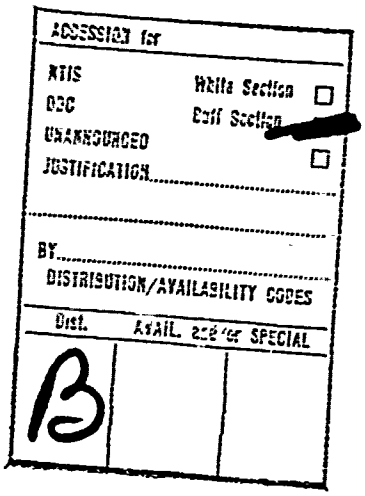


AIR FORCE WEAPONS LABORATORY
Air Force Systems Command
Kirtland Air Force Base
New Mexico 87117

When US Government drawings, specifications, or other data are used for any purpose other than a definitely related Government procurement operation, the Government thereby incurs no responsibility nor any obligation whatsoever, and the fact that the Government may have formulated, furnished, or in any way supplied the said drawings, specifications, or other data, is not to be regarded by implication or otherwise, as in any manner licensing the holder or any other person or corporation, or conveying any rights or permission to manufacture, use, or sell any patented invention that may in any way be related thereto.

DO NOT RETURN THIS COPY. RETAIN OR DESTROY.

AFWL-TR-72-118

# PRELIMINARY TESTS ON CELLULAR CONCRETE FOR SMALL-SCALE CRATERING STUDIES

Hans Engle
Dale E. Stephenson
University of New Mexico, CERF

TECHNICAL REPORT NO. AFWL-TR-72-118

## FOREWORD

This report was prepared by the University of New Mexico, CERF, under Contract F29601-72-C-0024. The research was performed under Program Element 61102H, Project 5710, Subtask SA 102, and was funded by the Defense Nuclear Agency (DNA).

Inclusive dates of research were June 1971 through March 1972. The report was submitted 16 August 1972 by the Air Force Weapons Laboratory Project Officer, Major Neal E. Lamping (DEV).

This technical report has been reviewed and is approved.

Neal E. Lamping
NEAL E. LAMPING
Major, USAF
Project Officer

Gerald G. Leigh
GERALD G. LEIGH
Lt Colonel, USAF
Chief, Facility Survivability Branch

William B. Liddicoet
WILLIAM B. LIDDICOET
Colonel, USAF
Chief, Civil Engineering Research Division

## ABSTRACT

Small-scale cratering experiments are being conducted by the Civil Engineering Research Facility with systematic variation in the parameters of the experiments, especially in the charge configurations and media employed in the test beds. Before cellular (foam) concrete could be used in the small-scale cratering studies, it was necessary to understand its behavior in specific cratering environments and to determine the reproducibility of the results. Therefore, to acquire this information, eight preliminary high-explosive shots were fired on foam concrete pads. These shots demonstrated that crater shapes and sizes, type and quantity of ejecta, and fracture patterns are reproducible, and that foam concrete is a suitable material for simulating weak, porous rock.

(Distribution Limitation Statement B)

CONTENTS

## ILLUSTRATIONS



## TABLES

# SECTION I

# INTRODUCTION

## 1. BACKGROUND

It has been found from cratering studies that the presence of a competent layer beneath the soil affects the crater size and related phenomena. The study of cratering in this type of geology is one of the objectives of the small-scale cratering studies being conducted at the Civil Engineering Research Facility.

For this study it was necessary to construct a layered test bed. The mismatch in strength and velocity between the layers in the test bed were to be similar to those found in nature. An examination of available materials was made and foam concrete* was found to have the desired characteristics for the competent, lower layer. An added advantage to foam concrete is its relatively low cost and ease of fabrication and emplacement. However, before it could be used in the small-scale cratering studies, it was necessary to study its behavior in specific cratering environments. The results of these studies are reported here.

## 2. OBJECTIVE

Preliminary testing for the small-scale cratering studies was conducted to evaluate the behavior of foam concrete in order to determine the feasibility of using this material to simulate the weak, porous rock in the experiments and to ascertain the reproducibility of the results.

## 3. SCOPE

This report is concerned with eight preliminary 1-lb high-explosive (C-4) shots on four pads of foam concrete to establish basic crater phenomenology associated with foam concrete and to determine the responses of this medium to various charge configurations which might be used in future small-scale cratering studies.

---

*Readers who desire more information about foam concrete are encouraged to consult references 1 through 4.

## SECTION II

## TEST PREPARATION

### 1. FOAM CONCRETE PAD CONSTRUCTION

The forms for three circular foam concrete pads were constructed from 1/4-in. plywood and were built on a leveled soil surface in the test area west of the Civil Engineering Research Facility, Area Y, Kirtland Air Force Base East. Soil was placed against the outer sides of the forms for lateral support. The form for a square foam concrete pad was fabricated from 1- x 12-in. boards and placed on asphaltic concrete.

A water-cement slurry was delivered in transit-mix trucks to the test site where additional water, if needed, was added. Then the foam mix was added to the water-cement slurry from a 30-gal pressure tank. The foam concrete pads were poured and allowed to cure for a minimum of seven days. Table I lists the shape and size of the pads, the composition of the foam concrete, and the dates on which the pads were poured.

### 2. TEST SAMPLES

Test cylinders, 6 by 12 in., were taken from each batch of foam concrete for strength, unit weight, void ratio, porosity, and ultrasonic velocity testing in the laboratory. Table II shows the results of these tests for the four foam concrete pads. On one test, cores were taken from the test slab to examine *in situ* properties.

### 3. CHARGE CONFIGURATIONS

The four charge configurations used in the testing of the foam concrete are shown in table III.

### 4. INSTRUMENTATION

Only shot 3 was instrumented. After pad 2 was poured, it was decided to measure the acceleration and velocity of shot 3 which was to be fired on this pad. Therefore, two 6-in.-deep channels were carved into the surface of the pad along perpendicular lines (N and W) to accommodate the instrumentation. Six piezoresistive accelerometers (Endevco Model 2264-30K-R), which have a maximum range of 30,000 g and a mounted resonant frequency of 90 kHz, were used. Three accelerometers were placed in each channel at 2, 3, and 4 ft from the center of the pad (fig. 1). Fresh foam concrete of the same proportion as the original pad was poured into the carved channels to hold the accelerometers in position.

Table I

FOAM CONCRETE PAD DATA

| Pad | Date Poured | Shape | Dia., ft | Depth, ft | Quantity, lb* | | | Water-Cement Ratio |
|---|---|---|---|---|---|---|---|---|
| | | | | | Water | Cement** | Foam | |
| 1 | 18 June 71 | Circular | 10.0 | 1 | 1586 | 2397 | 138 | 0.66 |
| 2 | 10 Sept 71 | Circular | 10.0 | 3 | 4522 | 7520 | 388 | 0.60 |
| 3 | 25 Feb 72 | Circular | 10.0 | 1 | 3388 | 5640 | 284 | 0.60 |
| 4 | 25 Feb 72 | Square | 9.5 | 2 | 3388 | 5640 | 284 | 0.60 |

*Quantities are based on delivery records.

**Type III Portland cement (high-early-strength).

Table II

FOAM CONCRETE PROPERTIES

| Pad | Compressive Strength, psi | Oven-Dried Unit Weight, pcf | Void Ratio | Porosity, % | Ultrasonic Velocity, ft/sec |
|---|---|---|---|---|---|
| 1 | 152.5*, 415.0** | 29.91 | 4.81 | 82.78 | 4919 |
| 2 | 189.0* | 31.78 | 4.29 | 81.09 | 5553 |
| 3 | 307.0*, 415.0** | 27.80 | 5.01 | 83.36 | 5508 |
| 4 | 415.0** | 27.80 | 5.01 | 83.36 | 5508 |

*Average of three 6- x 12-in. cylinders (10-day strength).

**Average of four 6- x 12-in. cylinders (19-day strength).

*Average of six 2- x 4-in. cores from the pad and six 6- x 12-in. cylinders (21-day strength).

**Average of six 6- x 12-in. cylinders (75-day strength).

Table III

CHARGE CONFIGURATIONS

| Shot | Pad | Configuration |
|---|---|---|
| 1 | 1 | Half Buried |
| 2 | 1 | Surface Tangent Above SGZ |
| 3 | 2 | Surface Tangent Above SGZ |
| 4 | 3 | Surface Tangent Above SGZ |
| 5 | 4 | Two Charge Radii Above SGZ |
| 6 | 4 | Two Charge Radii Above SGZ |
| 7 | 4 | Surface Tangent Below SGZ |
| 8 | 4 | Surface Tangent Below SGZ |

Note: SGZ = Surface Ground Zero.

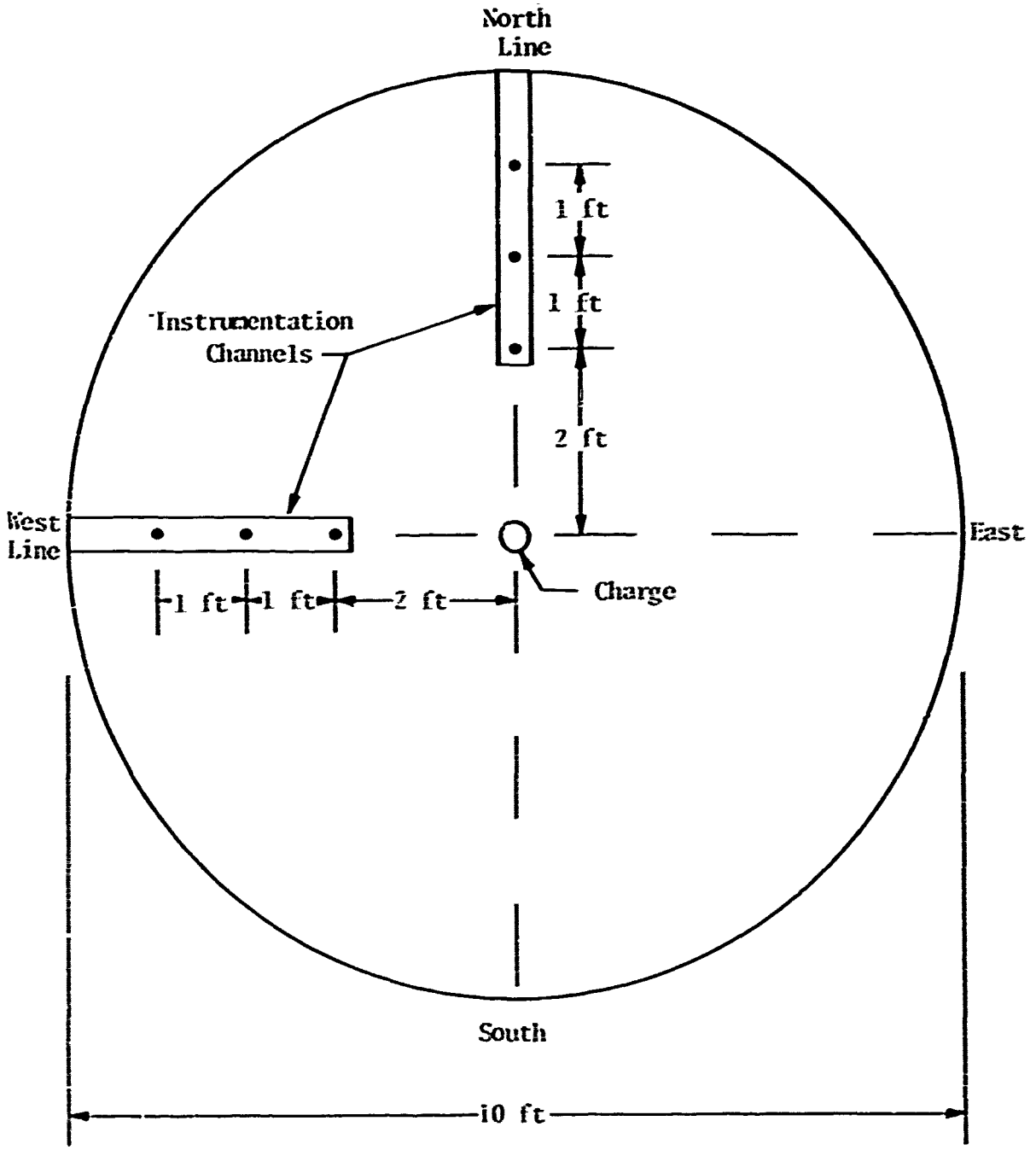


Figure 1. Location of Accelerometers on Pad 2

## SECTION III

## TEST PROCEDURES

### 1. FIRING OF EXPLOSIVES

In all tests, 1-lb spherical charges of C-4 explosive (TNT equivalent 1.5 lb) were fired by center detonation with M-1 electrical detonators (manufactured by R. Stresau Laboratory, Inc.). Shots 1, 2, and 4 through 8 were fired by a manually operated blasting machine; shot 3 was remotely activated by an automatic data acquisition system.

### 2. DATA RECORDING

Data from shot 3 were recorded on a United Electro Dynamics Inc. data acquisition system. Ampex CP 100 magnetic tape recorders operating at 60 ips with a band pass of 0 to 20,000 Hz were used in that system. An oscilloscope (Tektronix 502) and a Polaroid camera attachment were used for data display.

The true craters were determined by carefully removing the loose material produced by the shots. Crater measurements were made along eight radials from the center of the craters at 1-in. intervals of depth or range, depending upon crater shape (for kettle shape, depth was used; for all other shapes, range was used). Crater volumes on the circular pads were determined by graphical integration from profiles drawn in accordance with the above measured values. To check this method of determining the volume, the volume of the shot 3 crater was also measured by backfilling with a measured quantity of Ottawa sand (table IV). Crater volumes on the square pad (shots 5 through 8) were determined by the latter method only.

Surface fractures resulting from some shots were emphasized with black ink and recorded photographically.

Table IV

SUMMARY OF TEST DATA

| Shot Number | 1 | 2, 3, and 4 | 5 and 6 | 7 and 8 |
|---|---|---|---|---|
| Pad Number | 1 | 1, 2, and 3 | 4 | 4 |
| Charge Configuration |  |  |  |  |
| Crater Radius, in. | 10.00 | 7.25* | 8.10** | 12.00† |
| Crater Depth, in. | 9.50 | 7.80* | 5.40** | 13.25† |
| Crater Shape | Hemispherical | Kettle | Bowl | Cone |
| Shape Factor | 0.70 | 0.78* | 0.47** | 0.44† |
| Aspect Ratio | 1.05 | 0.93* | 1.50** | 0.90† |
| Measured Volume, $ft^3$ | -- | Shot 3: 0.465 | 0.296** | 1.525† |
| Integrated Volume, $ft^3$ | 1.200 | 0.590* Shot 3: 0.461 | -- | -- |
| Number of Radial Fractures | 9 | Shot 2: Interference Shot 3: Spalling (15) Shot 4: 9 | Interference Prior Cracking | Interference Prior Cracking |
| Ejecta — Quantity | Very Small | Very Small | Very Small | Small |
| Ejecta — Type | Up to 1/2-in. lumps | Up to 1/2-in. lumps | Up to 1/2-in. lumps | Up to 1/2-in. lumps |
| Impedance Mismatch | 1.25 | Pad 2: 1.49 Pad 3: 1.30 | 0.106 | 0.106 |

*Averaged data from shots 2, 3, and 4.

**Averaged data from shots 5 and 6.

†Averaged data from shots 7 and 8.

## SECTION IV

## RESULTS

The results from the foam concrete testing are limited here to passive elements such as the fracture patterns on the pads and the dimensions and shapes of the craters. The instrumentation data obtained from shot 3 may be found in reference 5.

### 1. HALF-BURIED CHARGE CONFIGURATION

The charge for shot 1 was half buried near the center of the northern half of pad 1. Figure 2 shows the resulting apparent crater which is nearly full of pulverized foam concrete and lumps of foam concrete, with very little ejecta on the pad. Upon removal of the powdered foam concrete, the true crater (fig. 3) appeared to be nearly hemispherical with a radius of 10 in., a depth of 9.5 in., and a volume of approximately 1.200 $ft^3$ (fig. 4). After sweeping the pad, nine distinct radial fractures which branched and zigzagged to the edge of the pad were revealed (fig. 5).

### 2. SURFACE-TANGENT-ABOVE-SGZ CHARGE CONFIGURATION

Three shots were fired in the surface-tangent-above-SGZ (Surface Ground Zero) charge configuration. As with the half-buried charge, there was very little ejecta produced and the craters were also nearly full of powdered and lumped foam concrete.

Shot 2 was fired near the center of the southern half of pad 1. Upon removal of the pulverized material from the crater, a kettle-shaped true crater (figs. 6,7) was disclosed in contrast to the nearly hemispherical shape produced by shot 1. Although evidence of radial cracks were noted, the fracture pattern was obscured by the fractures from the first shot. The true crater was 7.75 in. in radius and 8.75 in. in depth (maximum). Graphical integration of the field measurement profile (fig. 7) resulted in a volume of 0.689 $ft^3$. The previously noted radius and depth were also determined by using the field data.

Because of the interest developed by the unexpected and provoking kettle shape of the shot 2 crater and because two shots had been fired on the same 1-ft-thick pad, a second surface-tangent-above-SGZ shot (shot 3) was fired in the center of a new, 3-ft-thick pad (pad 2) to determine the reproducibility

Figure 2. Apparent Crater Produced by Shot 1

Figure 3. True Crater Produced by Shot 1

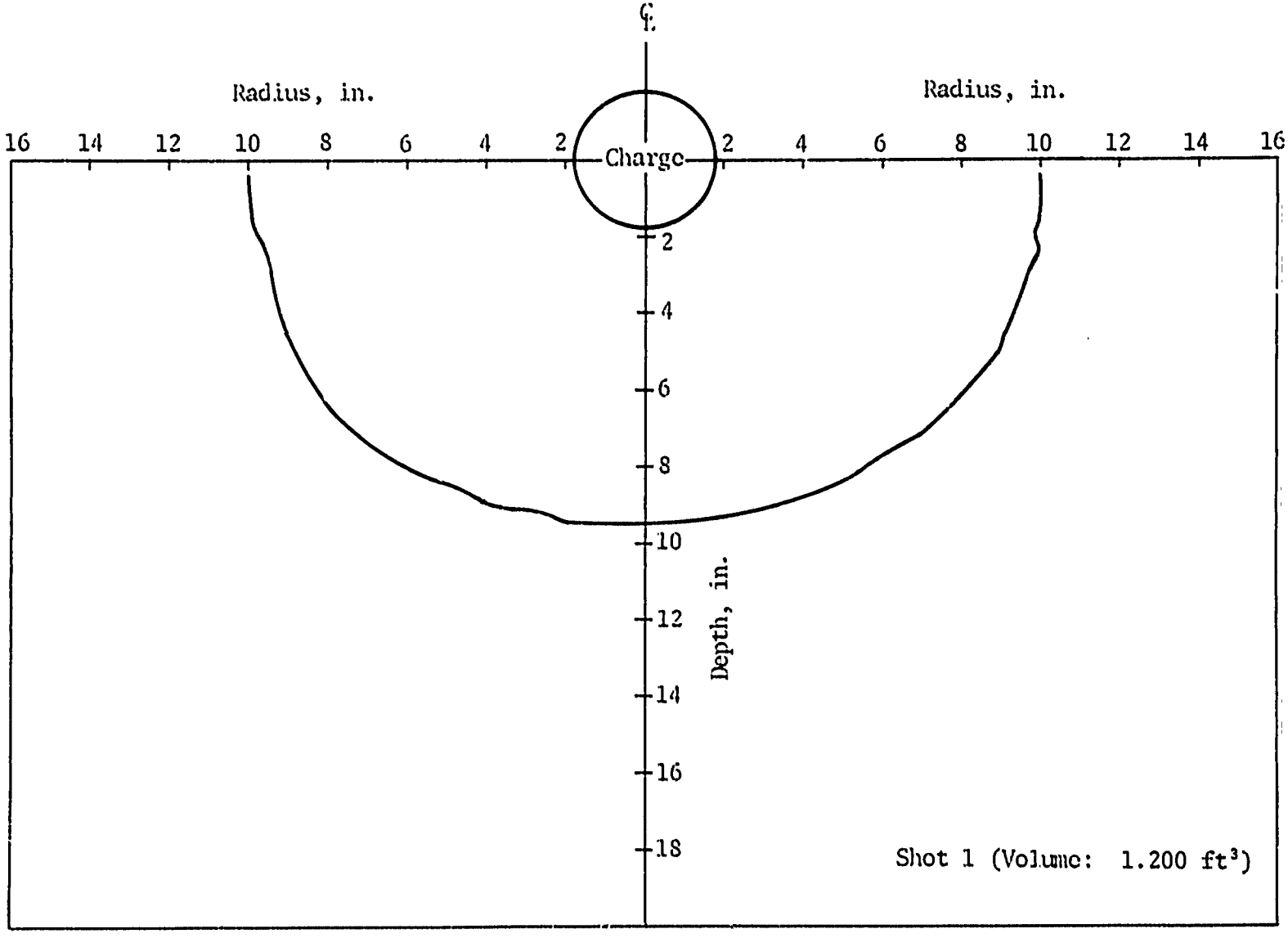


Figure 4. True Crater Profile for Half-Buried Charge

Figure 5. Radial Fracture Pattern Produced by Shot 1

Figure 6. True Crater Produced by Shot 2

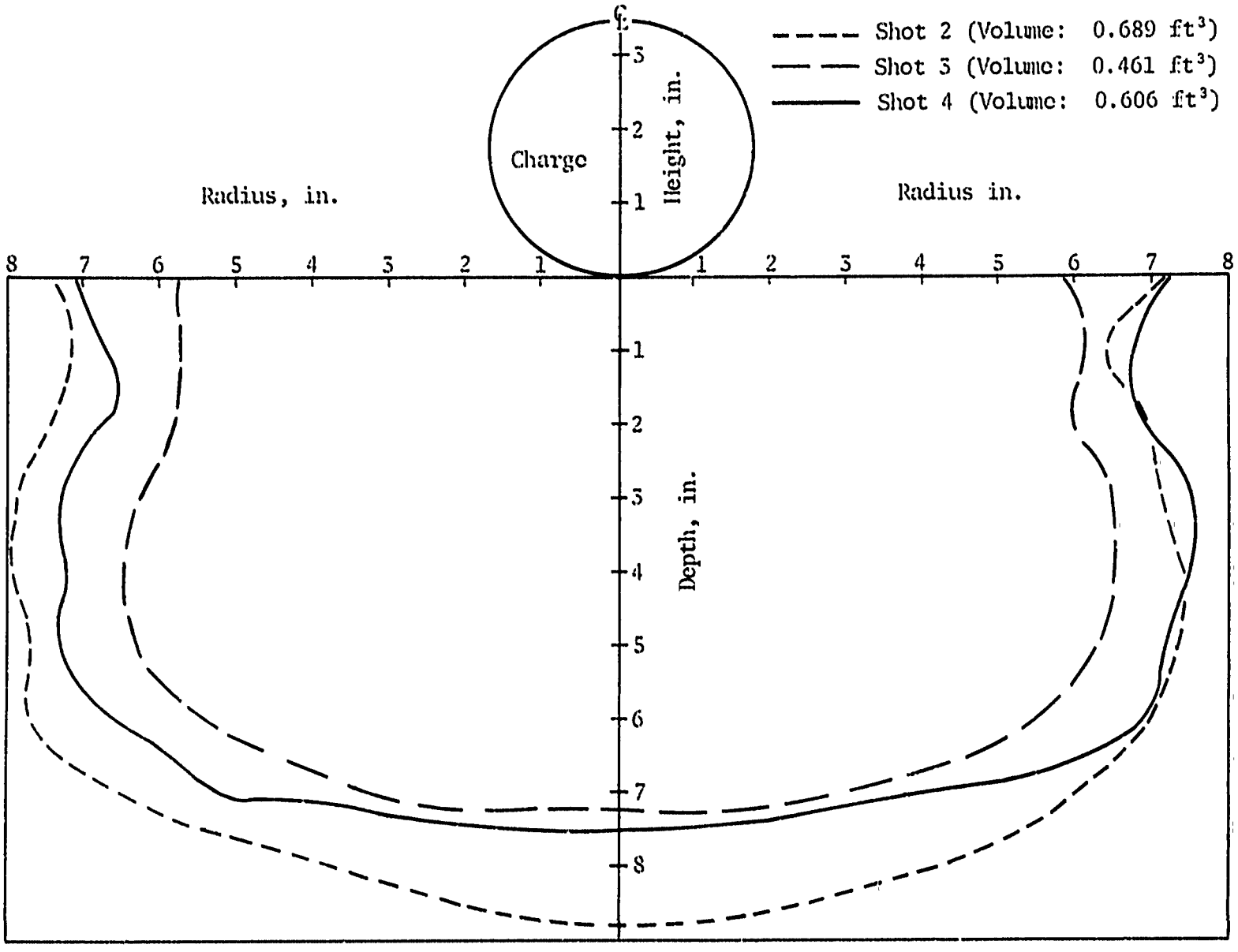


Figure 7. True Crater Profiles for Surface-Tangent-Above-SGZ Charge

of the results acquired from shot 2 and to obtain a distinct fracture pattern for the surface-tangent-above-SGZ charge configuration.

Preshot inspection of pad 2 revealed a hollow sound when the surface was tapped. This sound was due to the presence of air voids just under the surface. In addition, a faint, random fracture pattern, probably due to shrinkage, had developed on the surface of the pad.

Shot 3 reproduced the kettle-shaped true crater of shot 2 (figs. 7,8). It was also nearly full of crushed foam concrete, and again very little ejecta was produced. The radius, depth, and volume of this crater were 6.62 in., 7.25 in., and 0.461 $ft^3$, respectively. The postshot surface fracture pattern (fig. 8) appears to represent an enlargement of the preshot, random fracture pattern already noted.

The quadrant between the N and W lines of pad 2 was removed to obtain two vertical cross sections of the true crater and interior fracture patterns (fig. 9). The fractures near the side and base of the pad may be due to reflections

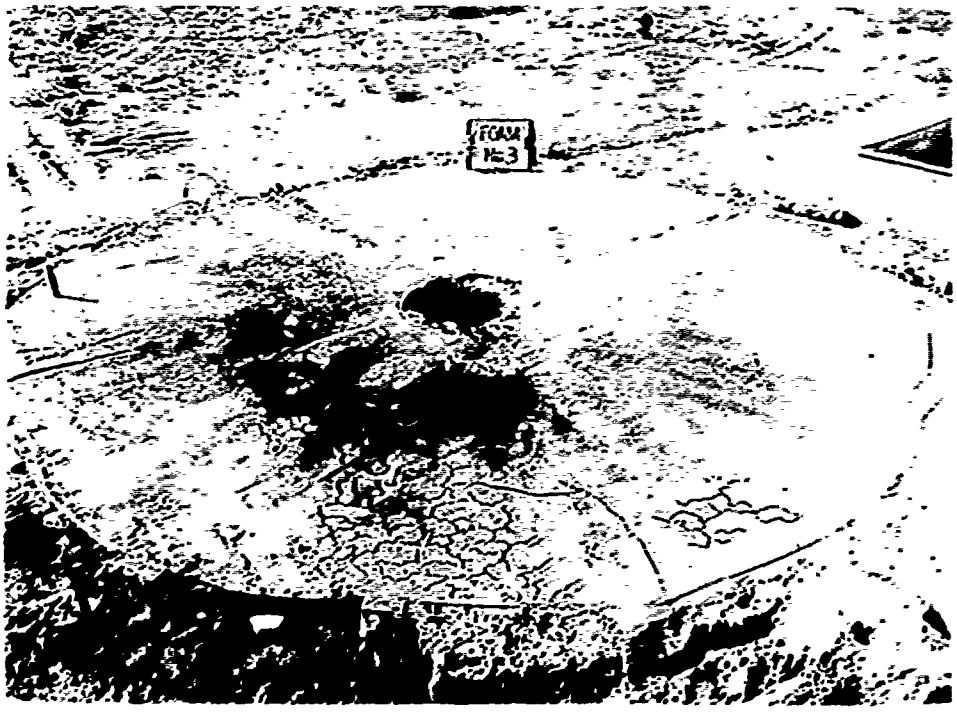


Figure 8. True Crater Produced by Shot 3

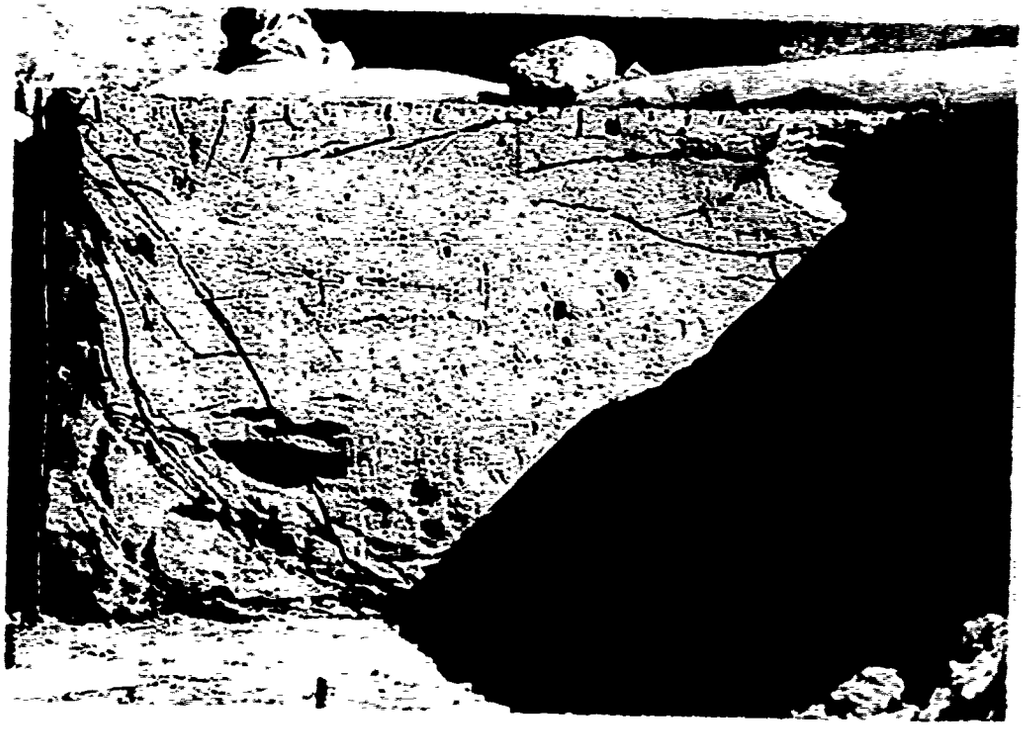

North Line

West Line

Figure 9. Cross Section of Pad 2 After Shot 3

of stress waves. Postshot examination revealed that some of the accelerometers were not completely embedded in the foam concrete. Figure 10 shows the thin surface layer (probably formed by the air voids noted above), the crater lip, and the fracture pattern within the pad including some prominent horizontal separations near the crater.

With the removal of the thin, randomly fractured surface layer, an irregular radial fracture pattern composed of mostly curvilinear cracks was uncovered (fig. 11).

A final surface-tangent-above-SGZ charge (shot 4) was fired on pad 3 to check the surface fracture pattern. This shot reproduced the kettle-shaped craters of shots 2 and 3 (fig. 7) and the radial fracture pattern of shot 1 (fig. 12). The shot 4 true crater had a radius of 7.38 in., a depth of 7.50 in., and a volume of 0.606 $ft^3$. The field measurement profile of this crater is shown in figure 7. The fracture pattern consisted of nine radial cracks which zigzagged to the edge of the pad; however, there was no discernible branching of the fractures as in shot 1. In addition, dark, radial patterns were observed on the surfaces of the pads on which the surface-tangent-above-SGZ charge was used (figs. 8,12). These patterns are probably caused by explosive products and may indicate lateral paths traveled by low-level ejecta.

### 5. TWO-CHARGE-RADII-ABOVE-SGZ CHARGE CONFIGURATION

Shots 5 and 6 (figs. 13,14) were fired on the southwest and southeast quarters of pad 4* with the charges suspended two charge radii above SGZ. The craters formed by these shots were filled with crushed foam concrete, and as in all the preceding shots very little ejecta was deposited on the pad. When the loose material was removed, nearly identical bowl-shaped true craters were revealed, indicating good reproducibility between the two shots. The radius, depth, and volume for the true crater of shot 5 were 8 in., 5.25 in., and 0.290 $ft^3$, respectively; the corresponding measurements for the true crater of shot 6 were 8.125 in., 5.50 in., and 0.302 $ft^3$, respectively. Volumes were determined by backfilling with Ottawa sand and measuring the volume of the sand.

These shots produced no readily identifiable, radial fractures or crack patterns on the surface.

*Several prominent horizontal and vertical fractures had developed on this pad by test time.

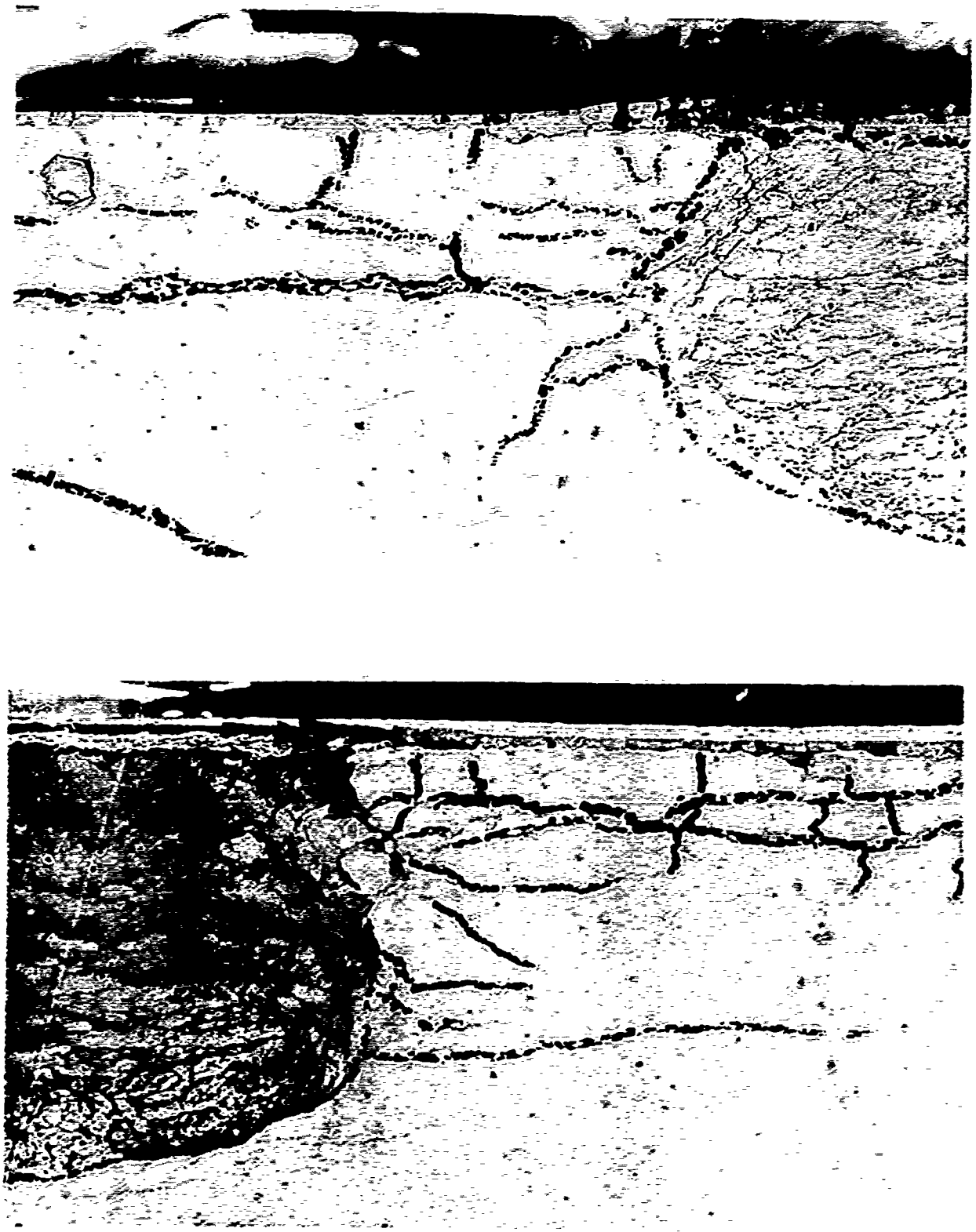

Figure 10. Shot 3 Fracture Details

Figure 11. Radial Fracture Pattern Produced by Shot 5

Figure 12. True Crater Produced by Shot 4

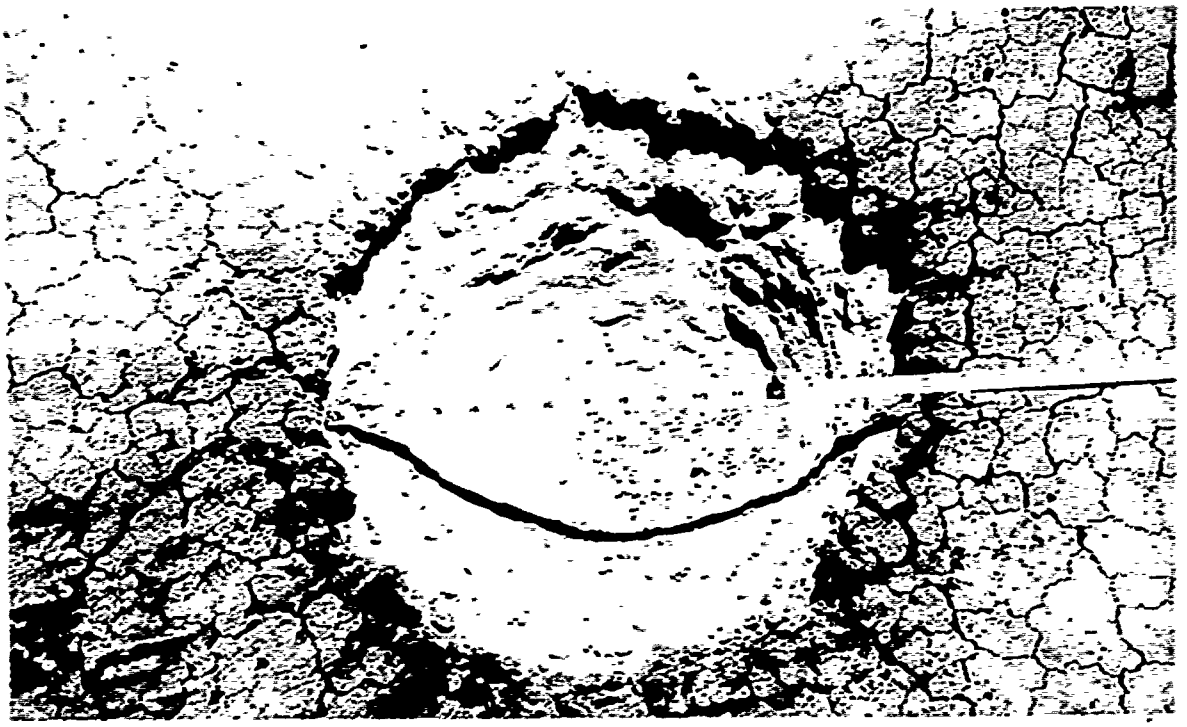

Figure 15. True Crater Produced by Shot 5

4. SURFACE-TANGENT-BELOW-SGZ CHARGE CONFIGURATION

Shots 7 and 8 were fired on the northwest and northeast quarters of pad 4 with a tangent-below-SGZ charge configuration. Holes were carved into the surface of pad 4 to receive these charges. Although still sparse, there was a little more ejecta thrown onto the pad than in the prior shots. The craters were nearly filled with crushed foam concrete. These shots produced cone-shaped true craters. (See fig. 15 for the apparent crater of shot 8.) The true crater radius, depth, and volume for shot 7 were 12 in., 15 in., and 1.470 $ft^3$, respectively. The corresponding measurements for shot 8 were 12 in., 15.5 in., and 1.580 $ft^3$, respectively (fig. 16). Volumes were again determined by backfilling with Ottawa sand and measuring the volume of the sand.

Both of these shots produced radial surface fractures; however, it was not possible to establish a definite crack pattern because of pre-existing fractures in pad 4.

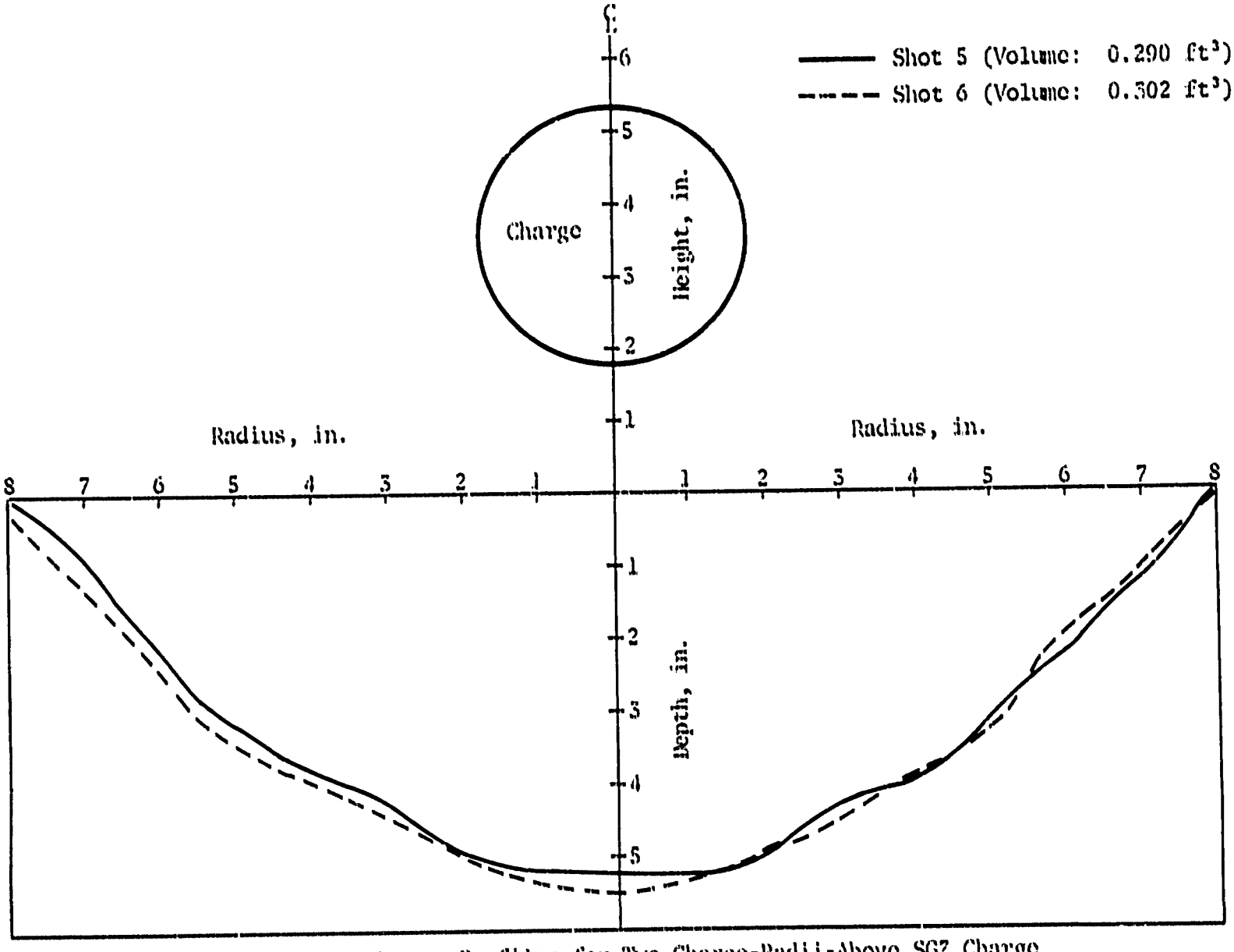


Figure 14. True Crater Profiles for Two-Charge-Radii-Above SG2 Charge

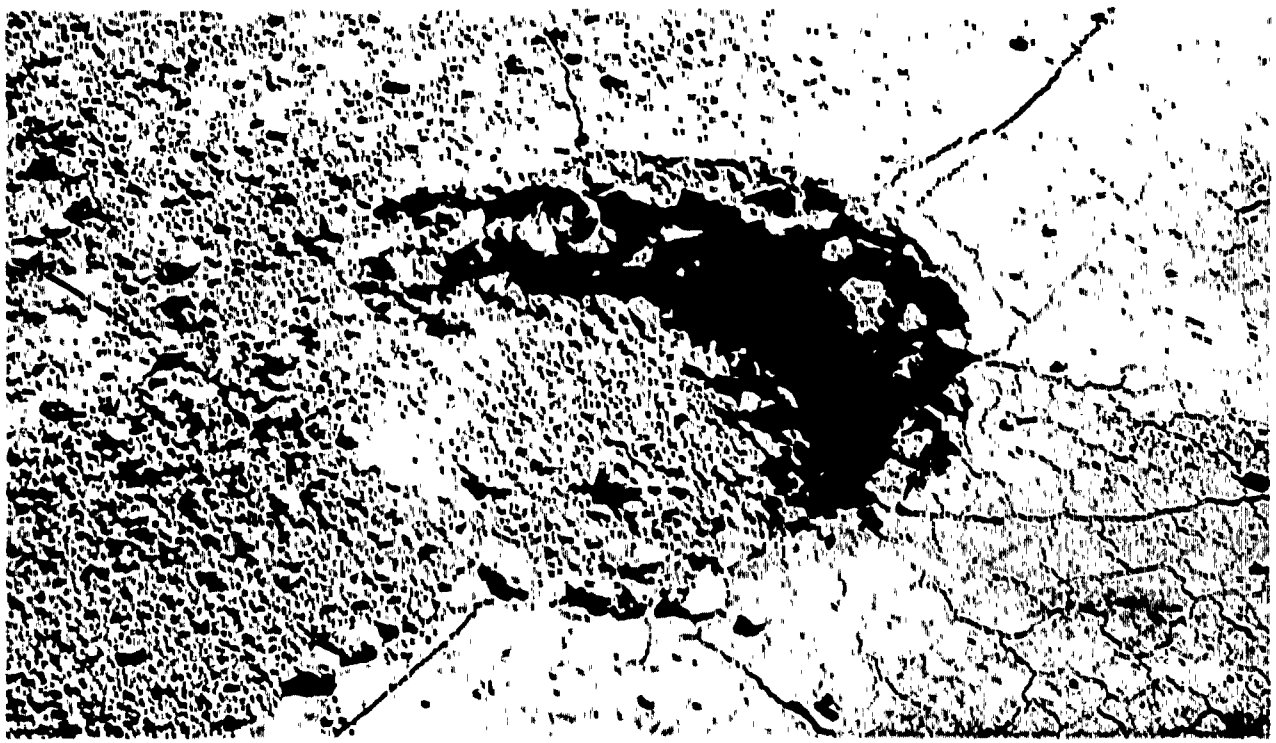

Figure 15. Apparent Crater Produced by Shot 8

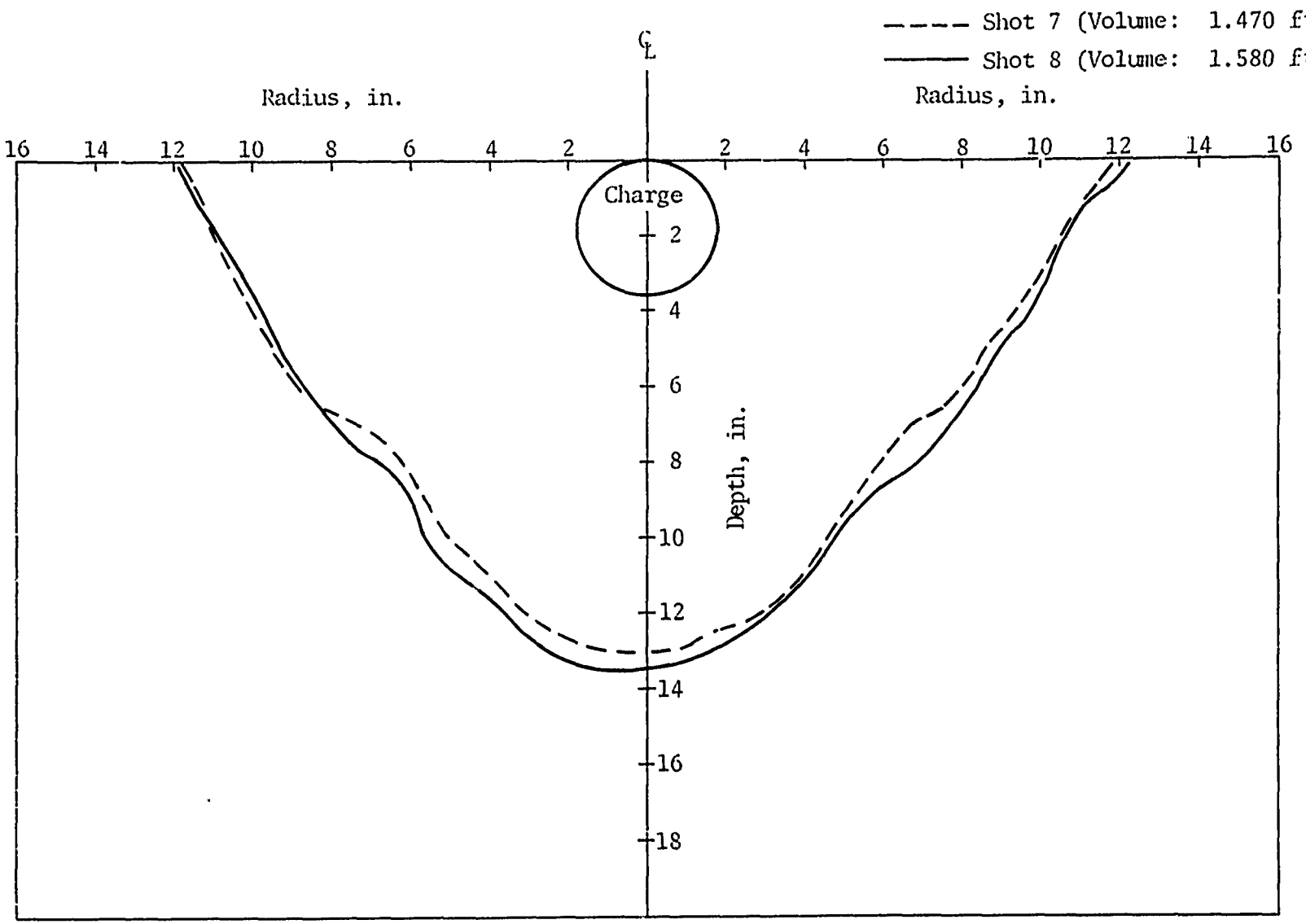


Figure 16. True Crater Profiles for Surface-Tangent-Below-SGZ Charge

## SECTION V

## DATA ANALYSIS

The results obtained from this preliminary series of tests to determine basic crater parameters in foam concrete are summarized in table IV. The crater shapes and sizes were very similar and reproducible for shots fired with the same charge configuration. Crater parameters from the three surface-tangent-above-SGZ shots (2, 3, and 4) varied the most--17 percent in radius, 21 percent in depth, and 50 percent in volume. Variations occurred between the test fired on pad 1 (shot 2) which was 1 ft thick and the test fired on pad 2 (shot 3) which was 3 ft thick. Shots 2 and 4 which were fired on pads 1 and 3, respectively (both were 1 ft thick) showed more nearly uniform parameters (fig. 7). Therefore, the greater difference in the crater sizes produced by shots 2 and 3 may be attributed in part to the difference in thickness of the two foam concrete pads. Shot 2 probably produced a larger crater than that produced by shot 3 because of the stronger wave reflection in the thinner pad which was due to the foam concrete/soil impedance mismatch. In addition, all shot 2 crater parameters were larger than those of shots 3 and 4. This is probably due to the lower strength of pad 1. (The lower strength of pad 1 resulted from the prior firing of shot 1 on this pad.) This is confirmed by the fact that the second shot of both the two-charge-radii-above-SGZ and the surface-tangent-below-SGZ charge configurations also had larger craters than the first shots. However, the differences in the size of craters between first and second shots of the same configuration on the same pad were not as great as the differences between the same type of shots on pads of different thicknesses.

Figure 17 shows crater volume, radius, and depth versus charge configuration for the 1-lb charges of C-4 in foam concrete. The volume curve seems to flatten out at the surface-tangent-below-SGZ point and appears to approach the optimum depth-of-burst. As would be expected, the crater depths and radii increase as the charge is lowered; however, optimum depth was not reached in these tests.

Fracture patterns consisting of nine radial cracks were produced by the half-buried charge in shot 1 and by the surface-tangent-above-SGZ charge in shot 4. Since the fracture pattern of shot 2 was superimposed on that of

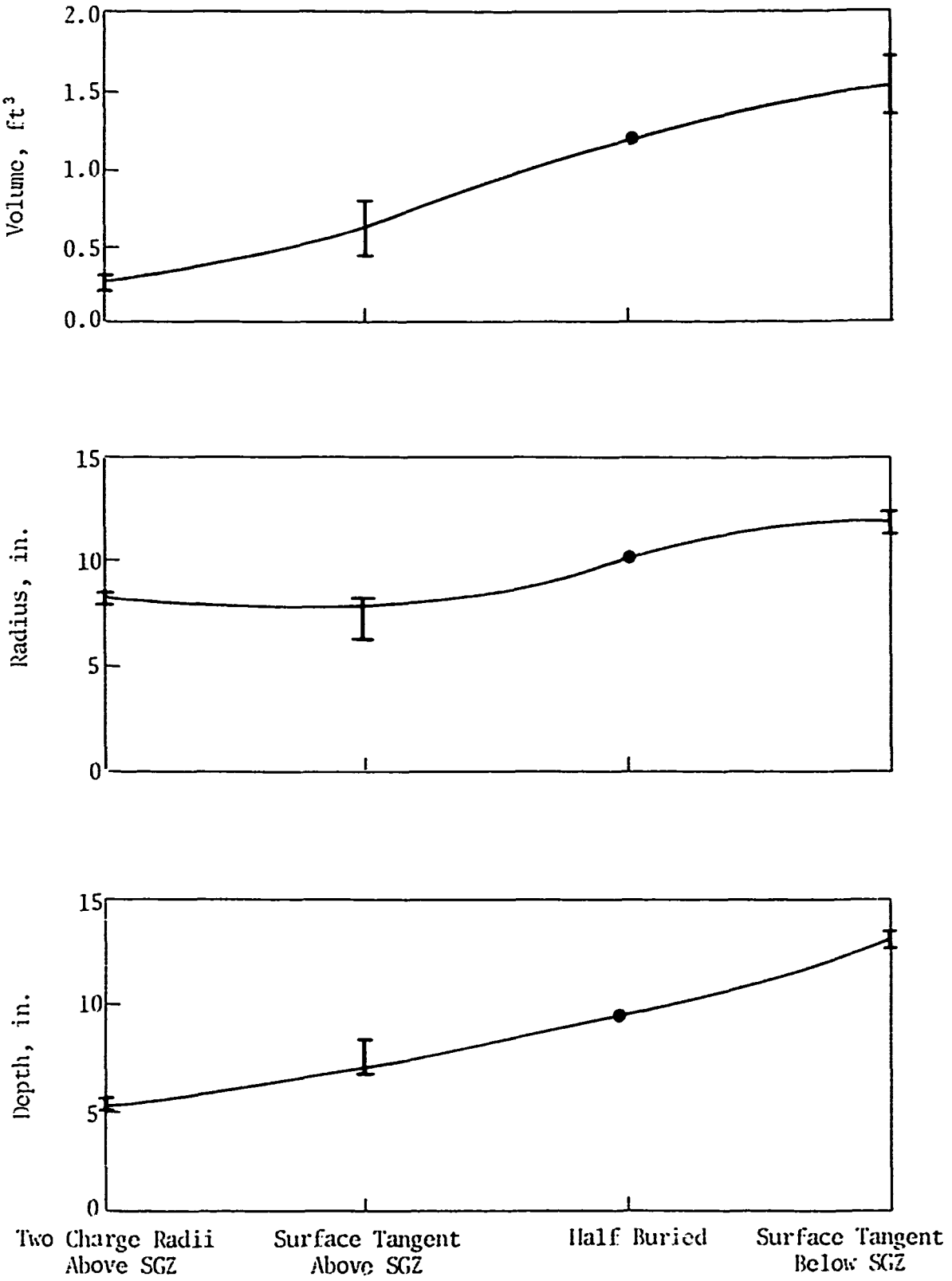


Figure 17. Crater Parameters versus Charge Configurations

shot 1 (on pad 1) it was indistinct. Although a radial fracture pattern was produced by shot 3, it differed from those of shots 1 and 4 in that there were about 15 curvilinear fractures which did not extend to the edge of the pad. These differences were probably due to heterogeneous foam concrete as evidenced by the presence of air voids under the thin surface layer. Some prominent horizontal fractures within the pad also pointed to an inconsistency in the foam concrete medium. No definitive radial fractures were produced by shots 5 and 6 (two-charge-radii-above-SGZ charge configuration); however, shots 7 and 8 (surface-tangent-below-SGZ charge configuration) produced several radial fractures. It was not possible to establish any definite fracture patterns for shots 5 through 8 because of pre-existing fractures in pad 4.

The most interesting result from this series of tests was the kettle-shaped craters resulting from the surface-tangent-above-SGZ shots. This shape resembled the pressure profiles from calculated surface bursts (ref. 5) or the Boussinesq solution of a concentrated normal load on a semi-infinite plate. It appears that these craters were formed by a spherical pressure wave produced by the detonation of the spherical charge. This wave crushed the foam concrete until attenuation reduced the pressure below its crushing strength and at the same time prevented most of the crushed medium from escaping as ejecta. This same hypothesis seems to apply to the other charge configurations.

# SECTION VI

# CONCLUSIONS AND RECOMMENDATIONS

## 1. CONCLUSIONS

The crater shapes resulting from all charge configurations (with the possible exception of the surface-tangent-below-SGZ shots) appear to have been formed by spherical pressure waves crushing the foam concrete until the wave strengths attenuated below the crushing strength of the medium. This crushing action probably kept most of the crushed foam concrete from escaping as ejecta. The largest quantity of ejecta was associated with the surface-tangent-below-SGZ shots due to some foam concrete being above the charge.

Tensile stresses were induced by all shots, producing some radial fractures which extended from the crater edges outward for various distances.

It is concluded from the results obtained that crater shapes and dimensions are reproducible in foam concrete; that this material behaves as a homogeneous medium under controlled conditions; and that foam concrete is suitable for simulating layers of weak, porous rock for future small-scale cratering studies.

## 2. RECOMMENDATIONS

It appears that foam concrete would be a suitable medium for studies combining theoretical calculations with experimental testing (ref. 5). In this connection, laboratory studies should be initiated to determine relevant properties and characteristics of this medium for use in computer codes. More instrumented shots should be planned which would lead to a better understanding of cratering phenomenology in foam concrete. It is especially recommended that the two-charge-radii-above-SGZ and the surface-tangent-below-SGZ shots be repeated under more closely controlled conditions. Testing with other charge configurations might prove rewarding, e.g., firing a charge below the optimum depth-of-burst to determine if a spherical cavity would be formed as the shots reported here seem to indicate.

## REFERENCES


1. "Design Manual," *Mearlcrete Concrete Roof Deck and Insulation* (typewritten book), Mearl Chemical Corporation, Roselle Park, New Jersey.

2. Valore, R. C., Jr., "Cellular Concrete, Part I," *Journal of American Concrete Institute*, Vol. 25, No. 9, May 1954, p. 773.

3. Valore, R. C., Jr., "Cellular Concrete, Part II," *Journal of American Concrete Institute*, Vol. 25, No. 10, June 1954, p. 817.

4. Linger, D. A., *Effect of Backpacking on Structure-Medium Interaction*, AFWL-TR-68-40, Kirtland Air Force Base, New Mexico, July 1968.

5. Cooper, H. F., Jr., and Shunk, R. A., *Some Preliminary Results from Small High Explosive Cratering Experiments on Foam Concrete*, AFWL-DE-TN-72-006, Kirtland Air Force Base, New Mexico, January 1972.

UNCLASSIFIED
Security Classification

## DOCUMENT CONTROL DATA - R & D

*(Security classification of title, body of abstract and indexing annotation must be entered when the overall report is classified)*

| | |
|---|---|
| 1. ORIGINATING ACTIVITY (Corporate author)<br>University of New Mexico, Civil Engineering Research Facility, Albuquerque, New Mexico 87103 | 2a. REPORT SECURITY CLASSIFICATION<br>UNCLASSIFIED<br>2b. GROUP |

3. REPORT TITLE

PRELIMINARY TESTS ON CELLULAR CONCRETE FOR SMALL-SCALE CRATERING STUDIES

4. DESCRIPTIVE NOTES (Type of report and inclusive dates)
June 1971-March 1972

5. AUTHOR(S) (First name, middle initial, last name)
Hans Engle; Dale E. Stephenson

| | | |
|---|---|---|
| 6. REPORT DATE<br>September 1972 | 7a. TOTAL NO. OF PAGES<br>31 | 7b. NO. OF REFS<br>5 |
| 8a. CONTRACT OR GRANT NO. F29601-72-C-0024<br>b. PROJECT NO. 5710<br>c. Subtask No. SA 102<br>d. | 9a. ORIGINATOR'S REPORT NUMBER(S)<br>AFWL-TR-72-118<br>9b. OTHER REPORT NO(S) (Any other numbers that may be assigned this report) | |

10. DISTRIBUTION STATEMENT
Distribution limited to US Government agencies only because test and evaluation information is discussed in the report (Sep 72). Other requests for this document must be referred to AFWL (DEV), Kirtland AFB, NM, 87117.

| | |
|---|---|
| 11. SUPPLEMENTARY NOTES | 12. SPONSORING MILITARY ACTIVITY<br>AFWL (DEV)<br>Kirtland AFB, NM 87117 |

13. ABSTRACT

(Distribution Limitation Statement B)
Small-scale cratering experiments are being conducted by the Civil Engineering Research Facility with systematic variation in the parameters of the experiments, especially in the charge configurations and media employed in the test beds. Before cellular (foam) concrete could be used in the small-scale cratering studies, it was necessary to understand its behavior in specific cratering environments and to determine the reproducibility of the results. Therefore, to acquire this information, eight preliminary high-explosive shots were fired on foam concrete pads. These shots demonstrated that crater shapes and sizes, type and quantity of ejecta, and fracture patterns are reproducible, and that foam concrete is a suitable material for simulating weak, porous rock.

DD FORM 1 NOV 65 1473

UNCLASSIFIED
Security Classification

| 14 KEY WORDS | LINK A | | LINK B | | LINK C | |
|---|---|---|---|---|---|---|
| | ROLE | WT | ROLE | WT | ROLE | WT |
| Cellular (foam) concrete | | | | | | |
| Cratering environments | | | | | | |
| Fracture patterns | | | | | | |
| Ejecta | | | | | | |
| Explosive cratering | | | | | | |